

Experimental study of mesoscopic fluctuations in nonlinear conductance and magnetoconductance

Roland Schäfer,* Klaus Hecker, and Helmut Hegger

II. Physikalisches Institut, Universität zu Köln, Zùlpicherstraße 77, D-50937 Köln, Germany

Wolfram Langheinrich

Institut für Halbleitertechnik der Technischen Hochschule Aachen, Sommerfeldstraße, 52056 Aachen, Germany

(Received 29 June 1995)

We investigate fluctuations in the differential conductance of a mesoscopic sample as a function of magnetic field and bias voltage. The sample consists of two funnel-shaped gold films connected by a narrow constriction. The cross section of the constriction is of the order of 5 nm^2 . This is extremely small compared to the elastic mean free path l in the adjacent larger portions of the structure. l is of the order of 50 nm. The conductance fluctuations (CF) are mainly due to diffusive motion of the conduction electrons in the wide regions of the gold film. In this respect the constriction probes via the CF the impurity configuration in the region of the gold film, which the electrons can explore coherently starting from a point within the constriction. Because of the smallness of the constriction, the size of the CF is smaller than the universal value predicted by theory by a factor of about 30. The fluctuation amplitude depends on the bias voltage. The dependence is in agreement with the theory of Larkin and Khmel'nitskiĭ. It can be studied in the magnetoconductance as well as in the conductance as a function of bias voltage for fixed magnetic field. A detailed analysis of the fluctuation amplitude yields identical values in both cases. This is in accordance with the ergodic hypothesis introduced by Lee and Stone. [S0163-1829(96)01523-8]

I. INTRODUCTION

At low temperatures the time over which conductance electrons in metals maintain their phase coherence, τ_φ , can exceed the elastic scattering time τ by several orders of magnitude.¹ The latter is via the Drude law simply related to the conductivity, $\sigma = ne^2\tau/m$. Here n is the electron density, e the elementary charge, and m the electron mass. However, the conductivity is only well defined as an average over length scales that exceed the phase coherence length L_φ considerably. L_φ measures the average travel distance of a conduction electron during the phase coherence time. Therefore the concept of conductivity, while extremely helpful in problems that involve metallic structures of larger size, loses its meaning in the so-called mesoscopic regime where one studies the behavior of samples with dimensions smaller than L_φ . In this regime the conductance is not a function of the conductivity and the sample geometry alone, but depends sensitively on the position of each single impurity. The Drude value of the conduction equals the mean value for the conductance over the locations of the impurities. But the conductance fluctuates significantly with the impurity configuration. For simple theoretical models the rms amplitude, $\text{rms}(G) = \langle (G - \langle G \rangle)^2 \rangle^{1/2}$ of the conductance fluctuations (CF) turns out to have a universal value of the order of e^2/h .^{2,3} If mesoscopic transport is diffusive the exact value of $\text{rms}(G)$ depends only weakly on the shape of the sample and does not depend at all on the degree of disorder in a wide range of impurity concentrations.

It is not hard to understand the origin of the conductance fluctuations. A conduction electron originally located at a given position within the sample spreads out during a time t over a spherical volume of diameter \sqrt{Dt} . Here D is the diffusion constant. It can reach every point within this dis-

tance on a great variety of random walks with the scattering centers as corner points. All the paths that lead to a specific point vary in length. This leads to a complicated interference pattern for the amplitude of the electronic wave function. It is essential that the phase coherence is maintained during the time period t . For $t \gg \tau_\varphi$ the probability density of the electron tends to be homogeneous. The same type of interference effect leads to a variation of the transmission probability of a conduction electron through a mesoscopic sample with the impurity configuration and hence to a variation of the conductance. While a naive expectation would be that these fluctuations are negligible due to the averaging over the tremendous number of possible paths, a careful analysis yields the universal conductance fluctuation (UCF) result. If a sufficient number of impurities is moved so that the length of all diffusive paths through the sample changes by a random amount of the order of the Fermi wavelength the conductance changes on average by the universal value of the UCF theory.⁴

It is clear that a change in every parameter that influences the phase of the electronic wave functions leads to CF as well. The most important parameter in this connection is probably the strength of the magnetic field. A change of the magnetic field changes the phase of each path by an amount $(2\pi/\Phi_0) \int \Delta A dl$, i.e., the phase change is proportional to the path integral over the change in the vector potential. $\Phi_0 = h/e$ is the flux quantum. CF were first observed as a function of the magnetic field.⁵ CF also occur as a function of the Fermi energy⁶ and of the applied voltage across the sample during the measurement.⁷ The connection between the fluctuations as a function of these external parameters and the fluctuations as a function of impurity configuration is established by an ergodic assumption put forward by Lee and Stone,² which will be discussed briefly in Sec. II.

One should keep in mind that the universal value of CF predicted by theory is barely observed in experiments. This is due to some drastic simplifications in the first theoretical model, which were, on one hand, necessary to obtain analytical results and, on the other hand, extremely helpful in putting forward our understanding of the physics of CF. In this model a disordered region of constant cross section is connected to exactly two particle reservoirs, which were kept on different chemical potentials to force a current to flow through the disordered region. So-called ideal leads connect the reservoirs with the disordered region. Within these leads no scattering of the electrons occurs at all. Thus, an electron once entered into the lead on one side will leave it on the other side in the same quantum state. The ideal leads separate the relaxation processes, which occur in the reservoirs and establish an equilibrium state there, from the purely elastic motion within the disordered region. The UCF theory as reported by Lee, Stone, and Fukuyama⁴ holds for this model. However, in the most common experimental method to measure a resistance four reservoirs are connected with real leads to the sample.⁸⁻¹⁰ Two of the reservoirs serve as a current source, while the remaining two are used to measure the resulting voltage drop across the sample. This classical method is known to eliminate the contribution of the leads to the total resistance. However, it is now well understood¹¹ that each additional lead and reservoir attached to a mesoscopic conductor influences the interference contribution. During the phase coherence time the electrons explore portions of the leads that are not part of the original sample. In addition, inelastic processes are introduced by allowing electrons to be substituted by electrons from the reservoirs that have no phase relation to the former ones. This leads to serious differences between the four-point measurement on one side and the theoretical results on the ideal two-point model. The size of the CF depends strongly on the separation of the voltage probes. The universal value of the CF predicted by theory is only observed if the separation of the voltage leads is equal to L_ϕ . One also finds asymmetries of the conductance with respect to the magnetic field that are actually in accordance with the Onsager relation but for the same reason are not present in the ideal two-lead model. Nevertheless, with a proper treatment of the additional features arising from two additional leads attached to a mesoscopic conductor, theory and experiment in four-point configuration seem to be in good agreement.^{8,10,11}

Further useful information has been obtained in configurations where only two leads are connected to a mesoscopic sample within a distance of L_ϕ .¹²⁻¹⁷ In these configurations the resistance of the leads has to be kept small compared to the mesoscopic sample itself to get meaningful information about the sample itself. This problem has been dealt with in two different approaches: Several groups¹²⁻¹⁴ have built a sandwich structure of two metallic layers with an insulating layer in between. The insulating layer contains a single hole of mesoscopic diameter. The resistance of this configuration is dominated by a mesoscopic volume around the hole. Another approach is to produce planar structures consisting of a homogeneous mesoscopic wire with one funnel-shaped contact on each end.¹⁵⁻¹⁷ The size of the contacts is large compared to L_ϕ . The whole configuration can be measured with the classical four-point method, but the resistance is mainly

due to the mesoscopic wire in the center, which is coupled only by two electrical connections to the outside world. In this case one finds CF in the magnetoconductance that are symmetric with respect to the magnetic field as expected for a two-point configuration. We have shown recently,¹⁷ by varying the length of the wire, that in this configuration a weak geometry dependence of the CF can be observed that is in good agreement with the theoretical predictions of the ideal lead model.

II. ERGODICITY

As mentioned in the Introduction, a change of the magnetic flux through the sample by an amount of the order of Φ_0 alters the conductance on average by the same amount as a rearrangement of the impurities. This is essentially the statement of the ergodic hypothesis introduced to the theory of UCF by Lee and Stone.² The rms amplitude of the CF in the magnetoconductance is equal to the rms amplitude of CF in the ensemble of different impurity configurations:

$$\langle \delta G^2(B = \text{const}) \rangle_{\text{ensemble}} = \langle \delta G^2(B) \rangle_B.$$

Here $\delta G(B) = G(B) - \langle G(B) \rangle$. The relation holds according to the hypothesis if the magnetic field is not too small. For zero magnetic field the ensemble fluctuations are expected to be larger⁴ by a factor of $\sqrt{2}$. It is worthwhile to mention that the CF in the magnetoconductance are much easier to observe experimentally than the CF as a function of impurity configuration. For the regime of large conductances $G \gg e^2/h$ the ergodic assumption could be proven by Al'tshuler, Kravtsov, and Lerner.¹⁸ An agreement within the experimental errors has been found experimentally, as well.¹⁹

UCF occur also as a function of Fermi energy and of the applied voltage across the sample.^{7,20} Both parameters influence the velocity of the electrons participating in the electronic transport so as to cause a phase randomization of the traversing electron trajectories. But the latter is much more difficult to treat theoretically because a study of nonlinearities in the voltage current characteristics excludes naturally the application of linear response methods. An analysis by Larkin and Khmel'nitskii²¹ indicates that the size of the fluctuations in the differential conductance $G_{\text{diff}} = dI/dU$ as well as in the conductance $G_{\text{int}} = I/U$ itself as a function of the bias voltage are expected to depend on the bias voltage. Experimental observations of CF in conductance versus voltage characteristics (G/V curves), on the other hand, show clear indications that the phenomena are not fully understood.^{22,23} From a straightforward expansion of the ergodic assumption by Lee and Stone² one would expect that an average over the magnetic field and over the bias voltage are equivalent to the ensemble average and thus equivalent to each other. But one encounters immediate difficulties. The average over the magnetic field is defined as

$$\langle \cdots \rangle_B = \lim_{B_{\text{max}} \rightarrow \infty} \frac{1}{2B_{\text{max}}} \int_{-B_{\text{max}}}^{B_{\text{max}}} dB \cdots \quad (1)$$

To calculate the rms amplitude of the magnetoconductance by means of this average is straightforward, because the size of the fluctuations is expected to be independent of the magnetic field (with the exception of a small field range close to zero magnetic field). To get a good estimate for the rms

amplitude one has to measure the fluctuations over a large field range. Since the size of the fluctuations in the G/V curves is not constant, a generalization to the case of the bias voltage is difficult. It is obvious that one cannot perform the limes operation in the definition of the magnetic field average [Eq. (1)]. This turns out to be in most cases the most limiting factor in the precision with which one can measure the rms amplitude. Similarly, one calculates the rms amplitude for the G/V curves in small voltage intervals. The intervals have to contain at least a couple of fluctuation minima and maxima. The rms value that one gets with a proper choice of the width of the averaging interval can be taken as a measure for the rms amplitude for the center of the determination interval. By sliding the determination interval over the full measuring range one gets a continuous function. For too narrow intervals this function is strongly fluctuating itself and thus a poor measure of the dependence of the rms amplitude, whereas for too large intervals the dependence is smoothed out. If the rms amplitude does not change too much over a single fluctuation period one can get in this way a fairly good estimate for the bias voltage dependence of the rms amplitude of the fluctuations in the G/V curves.

In summary we have two possibilities to determine the rms amplitude of the CF for a given dc voltage V_{dc} . We can average over the magnetoconductance trace and we can average over a small voltage interval around V_{dc} . In a generalization of the ergodic hypothesis introduced by Lee and Stone² we can expect to get the same value for the rms amplitude in both cases.

III. SAMPLE AND MEASUREMENTS

We report on measurements of CF obtained on a small bridge between two funnel-shaped contacts. The structure is made out of gold. The cross section of the bridge is considerably smaller than the elastic mean free path in the adjacent contacts. It is well known that in this case the resistance is dominated by the so-called Sharvin contribution,²⁴ which describes the resistance of a ballistic point contact and is given by

$$R_S = \frac{h}{e^2} \frac{2\pi}{Ak_F^2}.$$

Here A is the cross section of the point contact and k_F the Fermi wave vector. As common in the field of point contact spectroscopy, the cross section of the bridge is estimated using this formula. The resistance changed over the period of investigation (11 months) from 150 to 220 Ω . This yields a cross section of 8–5 nm².

The sample is produced by e -beam lithography and a lift-off technique. The procedure is described in detail elsewhere.²⁵ Our method is capable of reproducible structures down to 25-nm lateral size, but by chance we can get constrictions with considerably smaller size. Before the lift-off, a gold film of 30-nm thickness is evaporated on top of the structured polymethylmethacrylate- (PMMA-) based electron resist. The evaporation is done in a high vacuum chamber at room temperatures and gold with a purity of 99.999% is used. The mean free path in the resulting films at $T < 100$ mK has been measured to be typically 50 nm, corre-

sponding to a diffusion constant of $D \approx 220$ cm²/s. We use doped silicon as a substrate that is insulating at sub-Kelvin temperatures.

The sample is thermally coupled to the mixing chamber of a dilution refrigerator. The temperature was constant (± 5 mK) well below $T < 100$ mK. At this temperature the impurity configuration is fixed. This can be concluded from the reproducibility of the magnetoconductance fluctuations. The cross correlation of successive measured magnetofingerprints is usually larger than 80%. A small ac current ($I_{ac} = 250$ nA) of constant amplitude superimposed on a dc current I_{dc} that varies between plus and minus 100 μ A was applied. The ac part of the resulting voltage drop V_{ac} is monitored with a lock-in amplifier. $G_{diff} = I_{ac}/V_{ac}$ is a measure for the *differential* conductance. In this paper we discuss the differential conductance and omit from now on the subscript at G_{diff} . The differential conductance is a function of I_{dc} as well as of the magnetic field B . Since the observed conductance changes are at least smaller by a factor of 2×10^{-4} than the mean conductance it is convenient to calculate the dc voltage drop $V_{dc} = I_{dc}/G$ and we discuss G as a function of B and V_{dc} : $G = G(B, V_{dc})$. In this parameter space of G we have chosen two types of measurements. First, we measured the magnetoconductance for different values of fixed V_{dc} , $G(B, V_{dc} = \text{const})$. This we refer to as a magnetoconductance measurement. Then we measured G as a function of V_{dc} for different values of the magnetic field, $G(B = \text{const}, V_{dc})$. We call this a G/V curve in the following. The size of the CF does not depend on the temperature for $T < 100$ mK. The dependence for higher temperatures is discussed elsewhere.²⁶ In this paper we are only considering the low-temperature saturation value.

We were able to study the behavior of the sample over a period of 11 months. During this time seven cooling cycles were performed. In between the sample was stored at room temperature. While the fingerprints of the CF were stable as long as the sample was kept below $T = 100$ mK, uncorrelated fingerprints were observed after warming up to room temperature. This is due to the high mobility of defects in gold at room temperature and the high sensitivity of the CF to changes in the impurity configurations. But tempering of the sample at room temperature for a couple of months was even sufficient to alter considerably the mean conductance of the very sensitive device. While the first measurement yielded a conductance of $1/(150 \Omega)$ the conductance decreased during the period of investigation to $1/(220 \Omega)$. This corresponds to a decrease of the constriction dimensions. Most likely this is due to diffusion of some gold atoms into the silicon substrate. For the discussion of the results of our measurements it is of importance that the reduction of the conductance corresponds to a significant change in the sample geometry. While we have done all measurements at one single device, it nevertheless corresponds to a couple of different devices with slightly varying geometry. The overall behavior of the CF is preserved in all measurements and is therefore believed to be a common feature for mesoscopic two-point configurations in the nearly ballistic limit.

A. Magnetoconductance

Figure 1 shows examples for both types of performed measurements. The fluctuations are of the order of

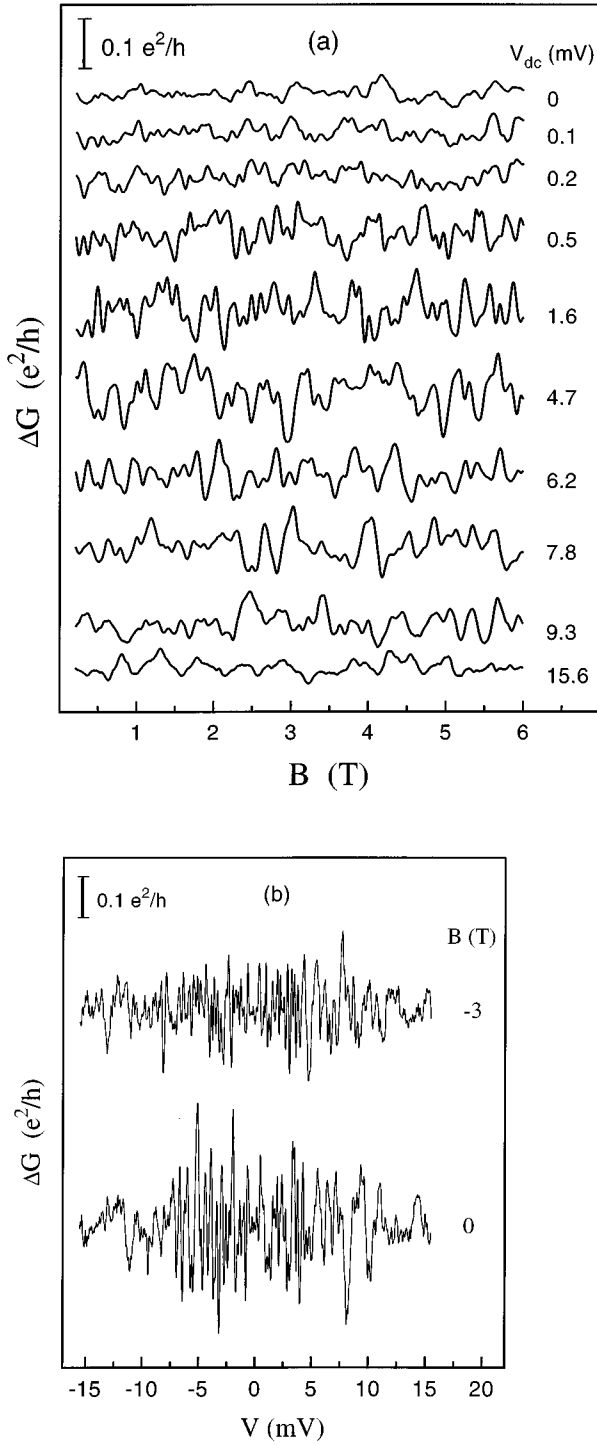


FIG. 1. (a) Magnetoconductance measurements for different dc voltages ($T < 100$ mK). (b) G/V curves for $B=0$ and 3 T.

$10^{-2} e^2/h$. This value is a factor of about 20 smaller than the universal value predicted by theory. A reduction of similar magnitude has been observed by Holweg *et al.*^{12,13} and can be attributed to the reduced return probability in ballistic constrictions. For a given magnetoconductance measurement the amplitude of the fluctuations is roughly constant as is obvious from Fig. 1. On the other hand, the rms amplitude of the fluctuations clearly changes with V_{dc} . As usual we get the amplitude of the magnetoconductance fluctuations from the maximum of the autocorrelation function

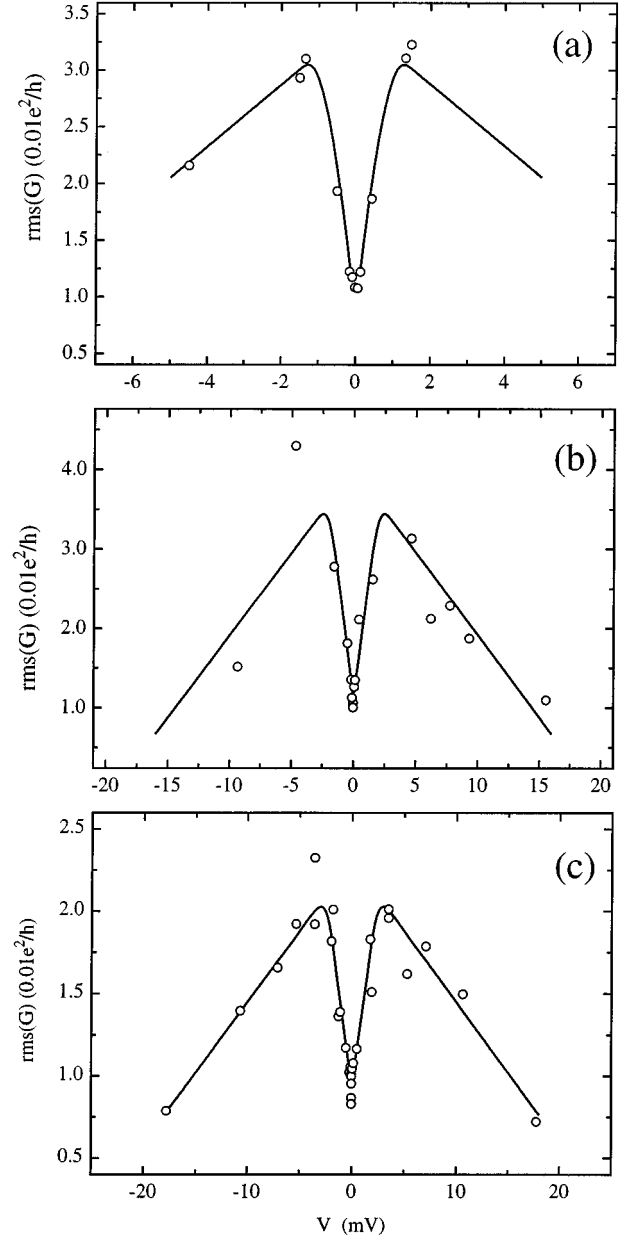


FIG. 2. $\text{rms}(G)$ vs V_{dc} extracted from the magnetoconductance measurements for three different cooling cycles. The lines serve to guide the eye. (a) Data from the first cooling cycle. $R=150 \Omega$. (b) Data from the second cooling cycle [after four months, evaluated from the data in Fig. 1(a)] $R=160 \Omega$. (c) Data from the third cooling cycle (after another three months) $R=180 \Omega$.

$$\mathcal{A}_G(\Delta B) = \frac{1}{2B_{\max}} \int_{-B_{\max}}^{B_{\max}} dB \delta G(B) \delta G(B + \Delta B).$$

Obviously $\text{rms}(G) = \sqrt{\mathcal{A}_G(\Delta B=0)}$. In Fig. 2 we show the result of the analysis for three different cooling cycles. The rms amplitude is small for zero dc voltage and increases considerably with increasing dc voltage. The solid curves are drawn as a guide to the eye. For higher dc voltages we find a decrease of $\text{rms}(G)$ resulting in a maximum for some intermediate values of V_{dc} . In the next section we show that the same behavior is found for the rms amplitude of the G/V curves and discuss it briefly. We point out that the magneto-

TABLE I. Cross correlation of G/V curves for different magnetic fields in %.

	50 mT	100 mT	150 mT	200 mT
0 mT	77	47	30	4
50 mT		60	40	12
100 mT			79	33
150 mT				55

conductance fluctuations are highly symmetric, showing the two-point character of our mesoscopic setup.

B. G/V curves

In Fig. 1(b) we show G/V curves taken at $B=0$ and 3 T. The CF are not symmetric with respect to V_{dc} and the rms amplitude depends on V_{dc} . The difficulties in determining the size of the CF in G/V curves is discussed in detail in Sec. II. We calculate the rms amplitude of overlapping portions of the G/V curves containing four minima and maxima. Such a small number of fluctuations within the determination interval ΔV_{dc} leads to a low resolution and is not fully satisfying. On the other hand, increasing ΔV_{dc} starts to smooth out the essential features of the rms(G) dependence. Therefore increasing ΔV_{dc} is inappropriate and an improved resolution can be achieved by averaging over the results for uncorrelated G/V curves. Two methods have been used to obtain uncorrelated G/V curves. The more time consuming one is to warm up the sample to ≈ 77 K between successive measurements. At these temperatures the impurity configuration changes due to the enhanced mobility of defects resulting in uncorrelated fluctuation patterns. More efficient is to change the magnetic field by an amount that exceeds the correlation field B_c considerably. In one cooling cycle we measured G/V curves for five different magnetic fields between 0 and 200 mT. The correlation between the different measurements is listed in Table I. Two fluctuation patterns taken at the same magnetic field are correlated to ≈ 89 %. For a field change of 50 mT the G/V curves are still highly correlated, but for a change of 100 mT the correlation has already dropped to 47%. In Fig. 3 we show the autocorrelation function of a magnetoconductance measurement. The autocorrelation function drops to half its maximum value for $\Delta B=96$ mT, in excellent agreement with the value obtained from the correlation of the G/V curves (Table I). The correlation scale of the G/V curves in Fig. 1(b) increases from a constant value of $V_c=80\pm 10$ μ V for bias voltages $V_{dc}<2$ mV to $V_c=150\pm 10$ μ V at $V_{dc}=10$ mV.

The averaged values of the rms amplitudes of the G/V curves for $B=0$ T and $B>0$ T are plotted in Fig. 4. We see that the fluctuations in G/V curves measured at finite field are considerably smaller than those measured at zero field. From the theory one expects a reduction of the rms amplitude of the fluctuations by a factor of $\sqrt{2}$.⁴ As soon as the magnetic field exceeds B_c we find no indication of a further dependence of the rms amplitude of the G/V curves on the magnetic field. For finite field we can use therefore uncorrelated G/V curves measured at different magnetic fields for the averaging procedure described above. To improve the

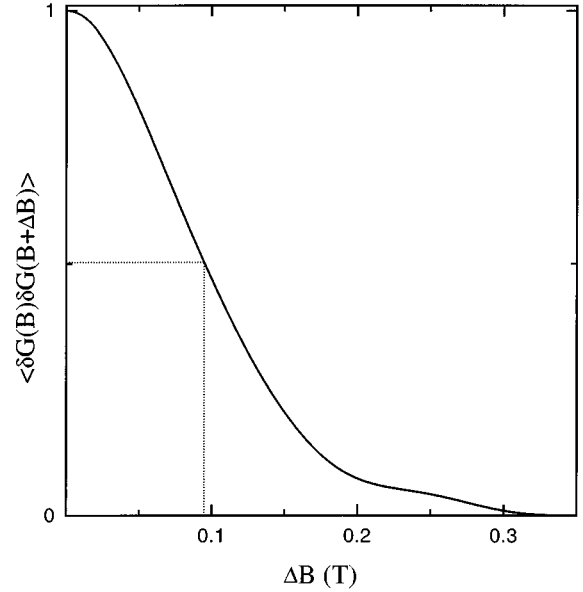


FIG. 3. Autocorrelation function of the magnetofingerprint $V_{dc}=0$ mV in Fig. 1(a). The half width $B_c=96$ mT defines the correlation field.

resolution for the data at zero field we have to average over results from uncorrelated G/V curves, which we get by thermally cycling the sample.

The closed dots in Fig. 4 represent the result of our complete analysis for finite fields while the open circles correspond to the results at zero field. As a guide to the eye we have drawn splines through the finite field data (lower solid curves), which summarize the common features of the results of the three cooling cycles. We get the upper splines by multiplying the lower ones by a factor of $\sqrt{2}$. They describe within the accuracy of our experiment the data obtained at zero field so as to confirm the theoretical expectation.

IV. DISCUSSION

In Fig. 5 we compare the data obtained from magnetoconductance measurements (Fig. 2) with the rms amplitudes estimated from the G/V curves in finite magnetic field (Fig. 4, lower curves). Figure 5 proves the equivalence of magnetic field and bias voltage averaging. It is important to notice, that we do not have a universal behavior of the CF. Their magnitude is much smaller than in the theory of UCF and they depend significantly on an external parameter, namely, the dc voltage. At zero bias voltage the rms amplitude of the fluctuations has the value $\text{rms}(G(B, V_{dc}=0)) \approx 0.01 e^2/h$, which is about a factor of 30 smaller than predicted by theory⁴ for a diffusive mesoscopic two-dimensional sample. A similar reduction has been found by other authors for quasiballistic point contacts.¹²⁻¹⁴ Nevertheless, both averaging mechanisms yield the same rms amplitude of the conductance fluctuations.

We now discuss briefly the behavior of the fluctuations in the differential conductance as a function of the dc voltage. Larkin and Khmel'nitskii²¹ (LK) have predicted an increase of the rms amplitude of the differential conductance with the applied bias voltage. In their introduction they give simple

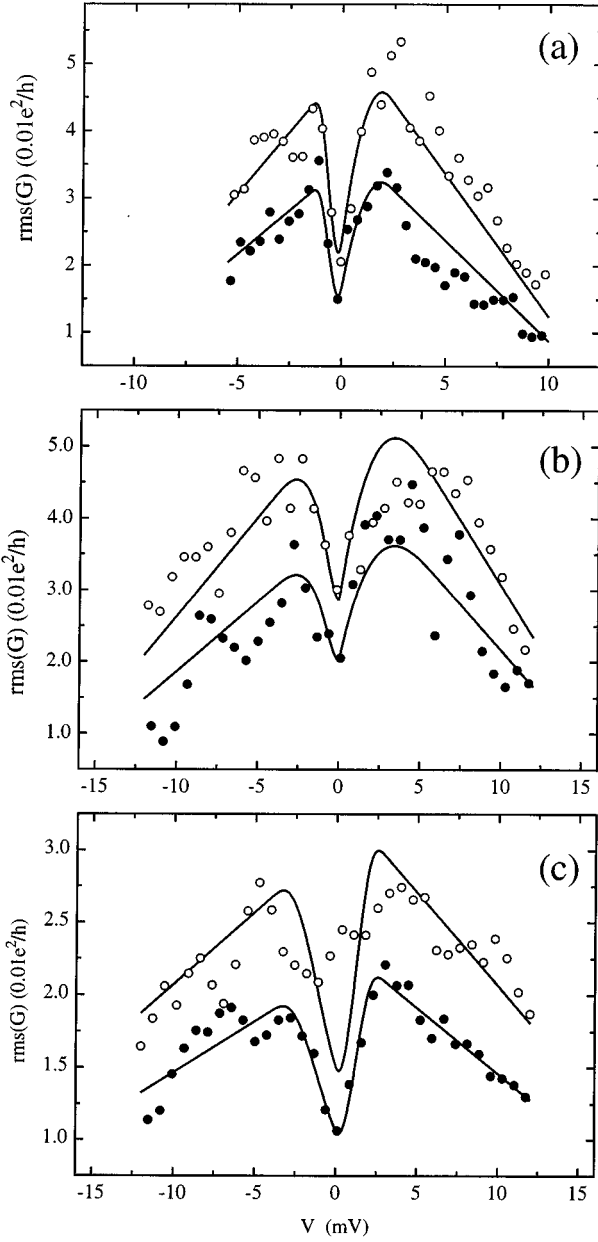


FIG. 4. $\text{rms}(G)$ vs V_{dc} extracted from the G/V curves. The closed dots represent the results for finite magnetic fields while the open circles corresponds to the results at zero field. The splines for finite field (lower curves) show the overall behavior of $\text{rms}(G)$. The upper lines are obtained by multiplying the lower ones by a factor of $\sqrt{2}$. The different parts of the figure correspond to the same cooling cycles as in Fig. 2. (b) is evaluated from the data in Fig. 1(b).

physical arguments that $\text{rms}(G) \propto \sqrt{V/V_c}$.²⁷ As the final result for the rms amplitude of the differential conductance using the diagrammatic technique of Keldysh they get

$$\begin{aligned} \text{rms}(G) &= \sqrt{K_g(V, \Delta V=0)} \\ &= \frac{1}{\pi} \frac{e^2}{h} \sqrt{\frac{V}{V_c}} \sqrt{\coth \frac{eV}{k_B T} - \frac{k_B T}{eV}}. \end{aligned} \quad (2)$$

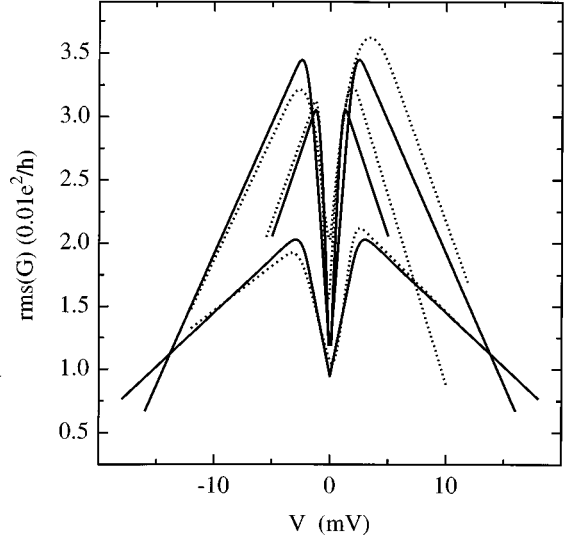


FIG. 5. Comparison of $\text{rms}(G)$ vs V_{dc} from Fig. 2 (solid line) and the finite field data of Fig. 4 (dotted line) showing the ergodic behavior of the fluctuations.

Here $K_g(V, \Delta V)$ is the correlator of the differential conductance. We observe an increase of the rms amplitude of the fluctuations with V_{dc} , which is in qualitative agreement with this theoretical prediction. The calculation of LK assumes a special geometry with $l/L \ll 1$. Here L is the length of the mesoscopic system. LK mention that the overall predictions of their theory will also hold for other geometries and ratios of l/L . So the exact voltage dependence of the fluctuation amplitude of our sample probably differs from Eq. 2. But the observed increase of the amplitude with V_{dc} is still expected.

In experiments of other authors^{7,14} the increase was not observed. This might be due to heating effects, which are caused by the high current density.²⁸ Heating leads to a strong decrease of both the phase coherence length and the thermal diffusion length $L_T = (hD/k_B T)^{1/2}$. L_T limits in addition to L_ϕ the distance over which the conduction electrons maintain their phase coherence. The decrease of the characteristic length scales leads to a reduction of the CF amplitude in contrast to the theoretical predicted behavior. Measurements of magnetoconductance fluctuations by Holweg *et al.*¹² at Ag point contacts showed an increase of $\text{rms}(G)$ with applied dc voltage up to $V_{\text{dc}} \approx 3$ mV but the authors did not discuss it.

In our case we are able to observe the increase because even for relatively large bias voltages the current density in the funnel-shaped contacts where those electron trajectories, which dominate the CF, are located stays low. This is the advantage of the almost ballistic motion in the region of high current density. In this region the electrons are rarely scattered and therefore cannot cause a rise of temperature. Only for higher dc voltages do we observe a decrease of the CF amplitude. For these voltages the large excess energy of the conduction electrons after acceleration by the electric field in the constriction leads to a generation of phonons and thus to a reduction of the phase coherence length. LK expanded their theory to higher voltages and temperatures and predicted a decrease of the amplitude of the fluctuations of the differential conductance due to inelastic processes.²¹

V. CONCLUSION

In this paper we report on measurements of fluctuations in the differential conductance of a small point-contact-like constriction in a mesoscopic gold structure as a function of magnetic field and applied bias voltage. The averaging procedure to obtain the rms amplitude was performed over both the magnetic field as well as over the bias voltage. The rms amplitude turned out to be a function of the bias voltage but within the experimental resolution we got the same value, regardless of the type of the average mechanism. We could

also confirm the $\sqrt{2}$ reduction of the rms amplitude of the fluctuations by a magnetic field.

ACKNOWLEDGMENTS

We gratefully acknowledge helpful discussions with G. Bergmann and E. Scheer. This work was supported by the Deutsche Forschungsgemeinschaft through SFB 341. One of us (R.S.) acknowledges financial support by the Deutsche Forschungsgemeinschaft.

*Present address: Forschungszentrum Karlsruhe, Institut für Nukleare Festkörperphysik, P.O. Box 3640, D-76021 Karlsruhe, Germany.

- ¹S. Washburn and R. A. Webb, Rep. Prog. Phys. **55**, 1311 (1992), and references herein.
- ²P. A. Lee and A. D. Stone, Phys. Rev. Lett. **55**, 1622 (1985).
- ³B. L. Al'tshuler, Pis'ma Zh. Éksp. Teor. Fiz. **41**, 530 (1985) [JETP Lett. **41**, 648 (1985)].
- ⁴P. A. Lee, A. D. Stone, and H. Fukuyama, Phys. Rev. B **35**, 1039 (1987).
- ⁵C. P. Umbach, S. Washburn, R. B. Laibowitz, and R. A. Webb, Phys. Rev. B **30**, 4048 (1984).
- ⁶J. C. Licini, D. J. Bishop, M. A. Kastner, and J. Melngailis, Phys. Rev. Lett. **55**, 2987 (1985).
- ⁷R. A. Webb, S. Washburn, and C. P. Umbach, Phys. Rev. B **37**, 8455 (1988).
- ⁸A. D. Benoit, S. Washburn, C. P. Umbach, R. B. Laibowitz, and R. A. Webb, Phys. Rev. Lett. **57**, 1765 (1986), A. D. Benoit, C. P. Umbach, R. B. Laibowitz, and R. A. Webb, *ibid.* **58**, 2343 (1987).
- ⁹W. J. Skocpol, P. M. Mankiewich, R. E. Howard, L. D. Jackel, and D. M. Tennant, Phys. Rev. Lett. **58**, 2347 (1987); H. Haucke, S. Washburn, A. D. Benoit, C. P. Umbach, and R. A. Webb, Phys. Rev. B **41**, 12 454 (1990).
- ¹⁰V. Chandrasekhar, P. Santhanam, and D. E. Prober, Phys. Rev. B **44**, 11 203 (1991).
- ¹¹M. Büttiker, Phys. Rev. Lett. **57**, 1761 (1986).
- ¹²P. A. M. Holweg, J. A. Kokkedee, J. Caro, A. H. Verbruggen, S. Radelaar, A. G. M. Jansen, and P. Wyder, Phys. Rev. Lett. **67**, 2549 (1991).
- ¹³P. A. M. Holweg, J. Caro, A. H. Verbruggen, and S. Radelaar, Phys. Rev. B **45**, 9311 (1992); P. A. M. Holweg, J. Caro, A. H. Verbruggen, and S. Radelaar, *ibid.* **48**, 2479 (1993),
- ¹⁴K. S. Ralls, D. C. Ralph, and R. A. Buhrman, Phys. Rev. B **40**, 11 561 (1989); D. C. Ralph, K. S. Ralls, and R. A. Buhrman, Phys. Rev. Lett. **70**, 986 (1993); K. S. Ralls, D. C. Ralph, and R. A. Buhrman, Phys. Rev. B **47**, 10 509 (1993).
- ¹⁵E. Scheer, H. v. Löhneysen, and H. Hein, J. Vac. Sci. Technol. B **12**, 3171 (1994).
- ¹⁶U. Murek, R. Schäfer, and W. Langheinrich, Phys. Rev. Lett. **70**, 841 (1993).
- ¹⁷K. Hecker, H. Hegger, R. Schäfer, U. Murek, C. Braden, and W. Langheinrich, Phys. Rev. B **50**, 18 601 (1994).
- ¹⁸B. L. Al'tshuler, V. E. Kravtsov, and I. V. Lerner, Pis'ma Zh. Éksp. Teor. Fiz. **43**, 342 (1986) [JETP Lett. **43**, 441 (1986)].
- ¹⁹D. Mailly and M. Sanquer, J. Phys. (France) I **2**, 357 (1992); N. J. Long, S. Yin, P. M. Echternach, and G. Bergmann, Phys. Rev. B **50**, 2693 (1994).
- ²⁰A. B. Fowler, A. Hartstein, and R. A. Webb, Phys. Rev. Lett. **48**, 196 (1982).
- ²¹A. I. Larkin and D. E. Khmel'nitskiĭ, Zh. Éksp. Teor. Fiz. **91**, 1815 (1986) [Sov. Phys. JETP **64**, 1075 (1986)].
- ²²P. G. N. De Vegvar, G. Timp, P. M. Mankiewich, J. E. Cunningham, R. Behringer, and R. E. Howard, Phys. Rev. B **38**, 4326 (1988).
- ²³H. Tang and Y. Fu, Phys. Rev. Lett. **67**, 485 (1991).
- ²⁴Y. V. Sharvin, Zh. Éksp. Teor. Fiz. **48**, 984 (1965) [Sov. Phys. JETP **21**, 655 (1965)].
- ²⁵W. Langheinrich, H. Beneking, U. Murek, C. Braden, and D. Wohlleben, J. Vac. Sci. Technol. B **9**, 2904 (1991).
- ²⁶R. Schäfer, Thesis, University of Cologne, 1993.
- ²⁷We point out that the rms amplitude of the conductance itself decreases with the bias voltage like $\sqrt{V_c/V}$. The conductance is defined as the total current divided by the bias voltage.
- ²⁸D. C. Ralph and R. A. Buhrman, Phys. Rev. B **49**, 2257 (1994).